CellPress

Developmental Cell
Resource

A Mesoscale Abscisic Acid Hormone Interactome Reveals a Dynamic Signaling Landscape in *Arabidopsis*

Shelley Lumba,[1] Shigeo Toh,[1] Louis-François Handfield,[2] Michael Swan,[1] Raymond Liu,[1] Ji-Young Youn,[3] Sean R. Cutler,[4] Rajagopal Subramaniam,[5] Nicholas Provart,[1] Alan Moses,[1,2] Darrell Desveaux,[1,*] and Peter McCourt[1,*]
[1]Cell & Systems Biology, University of Toronto and the Centre for The Analysis of Genome Evolution and Function, University of Toronto, Toronto, ON M5S 3B2, Canada
[2]Department of Computer Science, University of Toronto, Toronto, ON M5S 2E4, Canada
[3]Banting and Best Department of Medical Research, Terrence Donnelly Centre for Cellular and Biomolecular Research, University of Toronto, Toronto, ON M5S 3E1, Canada
[4]Botany and Plant Sciences, Chemistry Genomics Building, University of California, Riverside, Riverside, CA 92521, USA
[5]Agriculture and Agrifood Canada, 960 Carling Avenue, Ottawa, ON K1A 06C, Canada
*Correspondence: darrell.desveaux@utoronto.ca (D.D.), peter.mccourt@utoronto.ca (P.M.)
http://dx.doi.org/10.1016/j.devcel.2014.04.004

SUMMARY

The sesquiterpenoid abscisic acid (ABA) mediates an assortment of responses across a variety of kingdoms including both higher plants and animals. In plants, where most is known, a linear core ABA signaling pathway has been identified. However, the complexity of ABA-dependent gene expression suggests that ABA functions through an intricate network. Here, using systems biology approaches that focused on genes transcriptionally regulated by ABA, we defined an ABA signaling network of over 500 interactions among 138 proteins. This map greatly expanded ABA core signaling but was still manageable for systematic analysis. For example, functional analysis was used to identify an ABA module centered on two sucrose nonfermenting (SNF)-like kinases. We also used coexpression analysis of interacting partners within the network to uncover dynamic subnetwork structures in response to different abiotic stresses. This comprehensive ABA resource allows for application of approaches to understanding ABA functions in higher plants.

INTRODUCTION

Abscisic acid (ABA) is a sesquiterpenoid-based compound that has biological activity in a variety of organisms ranging from sponges and human parasites to mammalian cells in addition to plants (see Wasilewska et al., 2008 and Li et al., 2011 for review). In animals, for example, ABA appears to stimulate immune responses and insulin release from pancreatic cells. It has also been implicated in heat and light stress responses in animals. But the absence of a good model genetic system to study ABA in animals makes it difficult to understand the mechanisms underlying the role of ABA in mediating various responses. By contrast, in higher plants and particularly in the model *Arabidopsis thaliana*, functional analysis has shown ABA to be an important hormone in both embryonic and vegetative growth and development. In vegetative tissues, ABA protects plants from a variety of abiotic stresses such as drought, temperature, salt, and oxidative stresses (Nakashima and Yamaguchi-Shinozaki, 2013; Cramer et al., 2011). For this reason, the synthesis and signal transduction of ABA have been intensively studied not only at a fundamental level but also for potential applications in crop-based biotechnology (Ben-Ari, 2012; Wilkinson et al., 2012).

In higher plants, ABA appears to regulate both "fast responses" relating to ion channel flux in the guard cell and "slow responses" related to gene expression within the nucleus (see Hubbard et al., 2010 for review). Surprisingly genetic dissection of ABA signaling defines a relatively simple hierarchical signaling pathway that appears to regulate both responses (Figure 1A) (Cutler et al., 2010; Hubbard et al., 2010; Lumba et al., 2010). In the case of transcriptional responses, ABA binds to the PYR/PYL/RCAR (PYL) family of receptors, thereby allowing them to interact and inhibit a class of A-type protein phosphatase 2Cs (PP2Cs). PP2C inactivation permits a small set of class 3 sucrose nonfermenting-1-related protein kinase 2s (SNRK2s) to phosphorylate a collection of basic leucine zipper transcription factors (TFs) (ABA-responsive element binding factors [ABFs]). The phosphorylation of ABFs activates downstream gene expression through the *cis*-acting ABA response element (ABRE). ABA core components also directly regulate S-type anion channels SLAC1 and SLAH3 in the guard cell, demonstrating the core ABA signaling pathway also has cytosolic "fast response" targets (Geiger et al., 2011; Brandt et al., 2012).

Although the core signaling pathway illustrates the importance of ABFs in ABRE-dependent gene expression, the TFs that regulate the expression of the many other genes induced by ABA but lacking ABREs in their promoters have not been clearly defined. For example, up to 11 different TF families have been implicated in ABA-related processes (Fujita et al., 2011). Moreover, because of the role of ABA in protecting against various environmental stresses, the core ABA signaling pathway must work in coordination with signaling pathways involved in drought, heat, salt, and cold stress (Hey et al., 2010; Huang et al., 2012). The

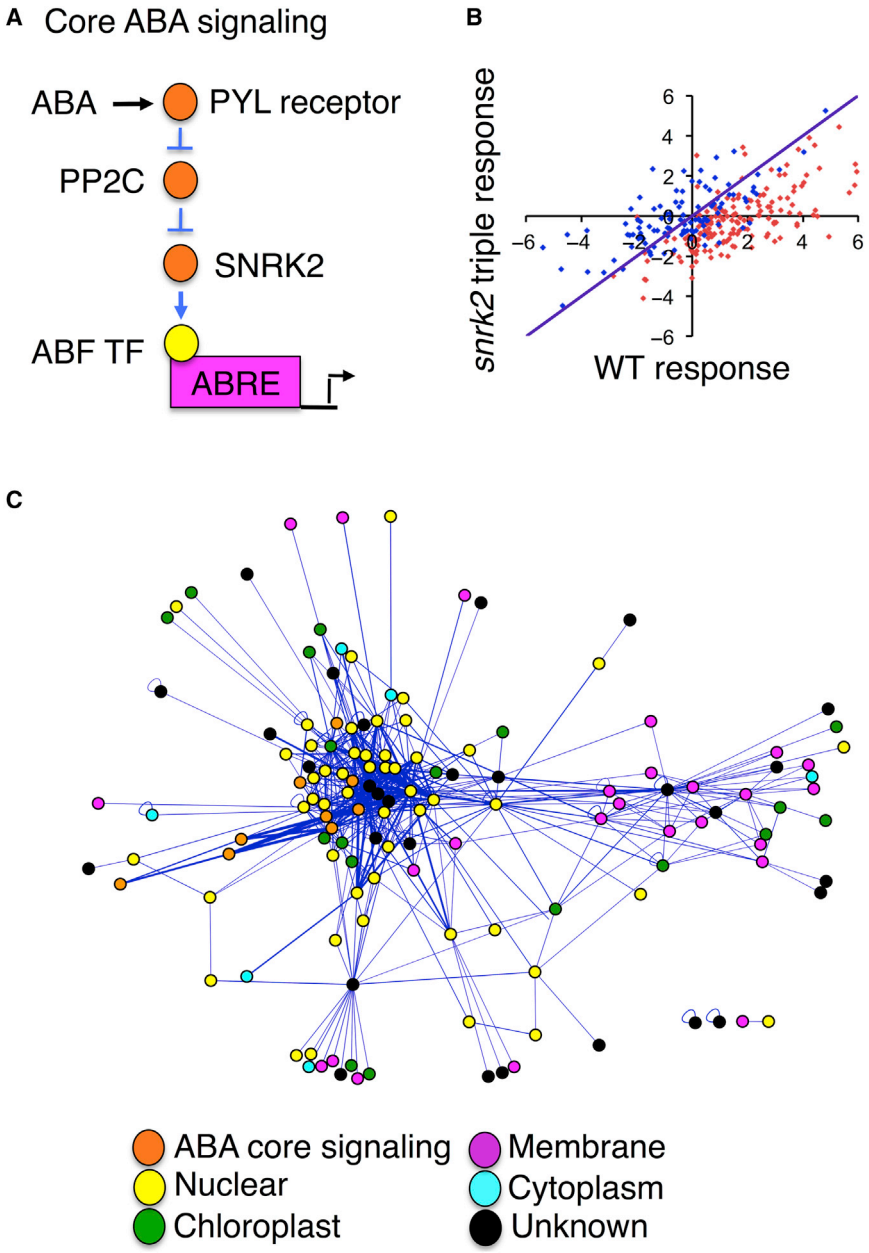

Figure 1. ABA Signaling Networks

(A) Model of core ABA signaling pathway as defined by genetic analysis. An arrow indicates positive genetic interaction, whereas a T-bar represents negative genetic interaction.

(B) A comparison of the expression of the 282set in wild-type (WT) seedlings exposed to 50 μM ABA for 6 hr versus the *snrk2* (*snrk2.2/2.3/2.6*) triple mutant defective in core ABA signaling. The red dots are genes induced at least 2-fold in the *aba2-2* mutant in response to ABA. Blue dots are genes repressed at least 2-fold by ABA. Gene expression below the purple diagonal line are dampened in induction in the *snrk2* triple, whereas genes above the diagonal line have increased expression. Graph axes are log-scale fold change.

(C) An edge-weighted force-directed representation of the TRAIN. Node color is designated by GO Slim Functional Annotation. Proteins with similar interaction profiles cluster more closely to each other. Line thickness represents edge-weighted confidence based on statistical analysis.

See also Figure S1 and Table S1.

overlap between primary ABA signaling and stress response pathways results in the formation of subnetworks that could reveal points of crosstalk and potential ways of modulating the ABA signal.

System-based approaches are beginning to be used to link signaling pathways into larger complex networks in plant biology (Van Leene et al., 2011; Arabidopsis Interactome Mapping Consortium, 2011; Lalonde et al., 2010). As networks become larger, however, interactions between components can quickly scale to a point where defining the roles of any particular protein is challenging (Hartwell et al., 1999; Spirin and Mirny, 2003). With these considerations, we used specific parameters to expand the components involved in ABA signaling while keeping the signaling network space experimentally manageable. We did this by first building a protein-protein interaction (PPI) network or interactome via yeast two-hybrid (Y2H) technologies in which the input gene set was limited to genes involved in the primary transcriptional response to ABA. Because PPIs occur more frequently within a group of coregulated genes than a randomly expressed gene set, this ABA-regulated gene set should be enriched for interacting protein partners (Ge et al., 2001). In addition, much of the core ABA signaling pathway is transcriptionally regulated by ABA, thus these core components provide a framework on which to expand the signaling network. Next, unlike many yeast-based interactome networks that use a single reporter system, we generated our ABA network using multiple reporter outputs and then integrated these outputs using machine learning algorithms and imaging software. This analysis allowed us to rank protein interactions based on statistically derived confidence levels.

This multilayered approach generated the "transcriptionally regulated ABA interactome network" (TRAIN) that encompassed over 500 additional PPIs of high quality. The TRAIN can be integrated with published protein interaction databases to build an expanded network (eTRAIN) of over 1,000 interactions. Our approach verified most of the published ABA-related interactions and expanded core ABA signaling by more than 50 proteins. The development of the TRAIN is a useful resource for plant hormone researchers. For example, because the interaction space is experimentally tractable, systematic and targeted functional analysis can be performed. As a proof of principle, we identified a 20-member subnetwork centered

around two SNRK3s that appears to negatively modulate ABA responsiveness. We also show the TRAIN can be used to examine the dynamic structure of protein networks in response to various abiotic stresses. By mapping stress-dependent coexpression of gene pairs over multiple time points and tissues, we were able to visualize how the wiring of the TRAIN subnetworks changed in response to specific abiotic stresses. We used this information to discover an important TF involved in *Arabidopsis* salt stress response.

RESULTS

The Transcriptionally Regulated ABA Interactome Network

To identify a collection of genes that were rapidly regulated by ABA, we performed whole-genome transcript profiling on an *Arabidopsis* mutant deficient in ABA synthesis (*aba2*) (Léon-Kloosterziel et al., 1996). The use of an auxotroph versus a wild-type plant not only avoided complications involving the plant's response to exogenous and endogenous ABA pools but also may sensitize the transcription of both major and minor genes in response to ABA application. Because we were using seedlings deficient in endogenous ABA, we could limit ABA exposure to low concentrations (1 μM) for a short duration (6 hr). In addition, both ABA-treated and untreated plants were exposed to the translational inhibitor cycloheximide to enrich for primary transcriptional events (Figure S1 available online). Using these experimental conditions, we identified 282 genes (282set) whose expression changed 2-fold or more in response to ABA versus untreated seedlings (Table S1). Within the 282set, we found that 85.2% and 60.2% of genes that were induced and repressed by ABA, respectively, are also identified in other ABA transcriptome studies, suggesting the 282set is a good representation of ABA-regulated genes (Table S1). Moreover, the ABRE promoter element was significantly overrepresented (125 of 282 genes, p value of 3.98×10^{-18}), and approximately 80% of the 282set genes were dampened in the *snrk2.2/2.3/2.6* triple mutant, which is defective in core ABA signaling (Figure 1B) (Fujita et al., 2009). Interestingly, although the 282set contained many well-characterized ABA-responsive genes, approximately 40% of the gene set fell below the 2-fold expression cutoff that is often the basis of hormonally based gene expression experiments, but followed the same trend of induction or repression by ABA, which suggests *aba2-2* did sensitize transcription to ABA treatment (Table S1). In summary, the 282set represented a transcriptionally sensitized gene set that is mostly regulated by the core ABA signaling pathway.

We next constructed a protein interaction map for 258 genes of the 282set based on a binary or an "all by all" Y2H approach (Table S1). Because ABA receptor-PP2C interactions are ABA dependent in yeast, all Y2H assays were performed in both the presence and absence of ABA to determine whether any of the 66,564 potential PPIs were dependent on ABA (Park et al., 2009). Therefore, this study represented a comprehensive analysis of ABA-dependent interactions. Larger scale Y2H analysis is often performed in series where autoactivating proteins are first identified using one reporter system, and then all subsequent interactions are retested using a different reporter system (Yu et al., 2008). We found, however, that protein autoactivation frequently depended on the reporter assay; thus, performing Y2H assays in series could result in a sampling bias that eliminates potential interactions only found in one reporter system. To reduce reporter bias, we performed Y2H assays using two reporter outputs in parallel. Although it is relatively easy to score interactions involving a colorimetric output (X-gal), the quantification of outputs based on yeast growth (growth in the absence of leucine) required the development of an imaging algorithm (DataEater) that did not require high-resolution images of yeast colonies (Supplemental Experimental Procedures). DataEater automatically generated a table of pixel intensities for each colony as a relative quantification of yeast growth. Using these values in combination with the X-gal data, we devised a simple generative model that assigned confidence values for each interacting pair that led to a list of 512 statistically significant PPIs involving 138 gene nodes (Supplemental Experimental Procedures and Table S1). This set of interactions represents approximately 0.8% of the possible interaction space.

The TRAIN contains genes that have functions in diverse processes ranging from metabolism and proteolysis to signaling and transcription (Figure 1C). A force-directed representation of the TRAIN in which proteins with similar interacting partners are more proximal while proteins with less similar interactions are positioned further apart revealed a dense cluster of protein interactions (Figure 1C). Gene ontology (GO) annotation suggested this cluster was enriched for proteins that localize in the nucleus, many of which are TFs. Furthermore, this dense region also contained a number of core ABA signaling components, including PYL receptors, PP2Cs, and ABFs, all of which are thought to have roles in the nucleus. Thus, many of the PPIs identified were not only ABA dependent for coexpression but also encoded nuclear proteins. Enrichment in protein pairs annotated with common GO is a common criterion for high-quality and biologically significant interactome data sets (Stelzl et al., 2005). In summary, the TRAIN fulfills many of the standard validation requirements commonly used in interactome studies.

The eTRAIN

The TRAIN is obviously not an exhaustive network because it is biased toward ABA-regulated gene expression. We therefore expanded the interactome by querying TRAIN proteins against three large protein interactome databases and a collection of literature-curated interactions (Arabidopsis Interactome Mapping Consortium, 2011; Lalonde et al., 2010; Popescu et al., 2009). This analysis expanded the TRAIN to a network of 573 proteins that encompassed 1,008 interactions and was designated the eTRAIN (Figure 2). The eTRAIN not only demonstrated the complex relationship of ABA signaling with respect to diverse biological processes but also suggested potential interplay between ABA and these other processes. For example, 31 genes within the eTRAIN were GO annotated as having roles in other hormone signaling pathways, and these nodes show approximately 100 interactions within the eTRAIN (Figure 2). These hormone-based nodes may act as points of crosstalk that help coordinate ABA with other hormonal responses.

Core ABA Signaling Network

Presently, core ABA signaling is composed of 13 PYL receptors, 9 PP2Cs, 3 SNRK2s, and 5 ABF transcriptional activators (Cutler

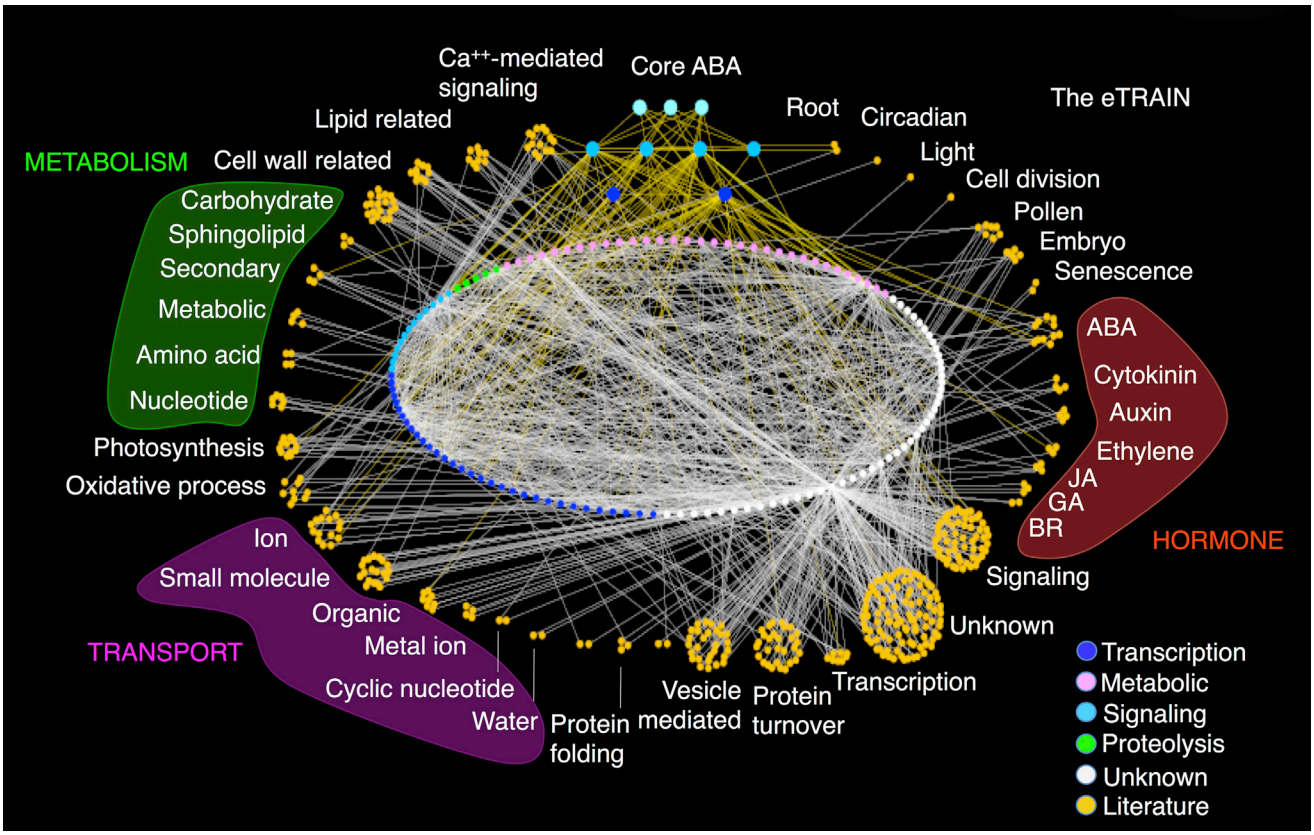

Figure 2. eTRAIN: An Expanded Map of ABA Signaling PPIs

Core ABA signaling components are represented by larger nodes at the upper center of the map, whereas TRAIN components are represented by nodes in the middle ellipse. Core and TRAIN node component colors are designated by GO Slim Functional Annotation. Literature-reported interactions are shown on the outside as orange nodes. Orange edges indicate interactions with core components. Categories shown on the outside are designated by GO Slim Functional Annotation. JA, jasmonic acid; GA, gibberellic acid; BR, brassinosteroid. The list of genes and interactions can be found in Table S1.

et al., 2010; Hubbard et al., 2010). The TRAIN consists of three *PYL* receptors (*PYR1*, *PYL4*, *PYL8*), four *PP2Cs* (*ABI1*, *AHG3*, *HAB1*, *HAI1*), two *ABFs* (*ABI5*, *ABF3*), but not *SNRK2* kinases, because the latter are not induced by ABA addition (Fujita et al., 2009; Fujii and Zhu, 2009). Of the 12 possible TRAIN-related PYL-PP2C interactions, 11 were recapitulated and no other interactions were found to be ABA dependent (Figure S2). We also identified previously reported interactions (PYL8/MYB77, AFP2, ABI5/AFP4), suggesting that our interaction conditions and statistical filtering were of high quality (Arabidopsis Interactome Mapping Consortium, 2011; Garcia et al., 2008).

In addition to these published interconnections, interactions among core proteins were identified between PP2Cs (ABI1/HAI1, AHG3/HAI1) and between PP2Cs and ABFs (ABI1/ABI5, HAI1/ABI5) (Figure 3A). These interactions are consistent with reports of interactions and direct dephosphorylation of select ABFs by various PP2Cs (Lynch et al., 2012). We also uncovered additional connections between the PYL8 receptor and the TFs MYB49 and a basic-helix-loop-helix (bHLH) (At1g10585) that we have designated as AIB1 for ABA-induced basic helix-loop-helix (Figure 3A). In addition, PP2Cs were found to interact with kinases (SNRK3.15, SNRK3.22, MAP3Kδ4), a phosphatase (SSP4), a large set of TFs, metabolic enzymes, and proteins of unknown function (Figure 3A). The PP2C interactions with SNRK3.15 and SNRK3.22 add to the large number of core PP2C-SNRK3 family interactions that already exist in the literature and further support the interplay between these ABA-regulated phosphatases and these calcium-regulated kinases (Batistič et al., 2012; Coello et al., 2011). Finally, ABFs were found to interact with the following: two kinases (MAP3Kδ4, WNK2), a phosphatase (SSP4), seven TFs (ABA-responsive NAC [ANAC]19, ANAC32, ANAC72, ERF58, CIR1, MYB49, AIB1), and a collection of proteins involved in metabolism and unknown functions (Figure 3A).

Functional analysis using sensitivity to ABA as a phenotype has been useful in classifying genes as positive or negative regulators of the overall ABA response. Literature curation of the components that touch core signaling proteins indicate eight genes encode positive regulators and 14 are negative (Figure 3A). To expand this functional analysis, we arbitrarily identified loss-of-function mutations for 16 TRAIN genes that interacted with core PP2Cs and determined their ABA sensitivity at the level of germination and cotyledon expansion (Figure 3B). Among the TRAIN genes, *myb12*, *athb12*, *erf58*, *rap2.2*, and *map3kδ4* all showed increased sensitivity to ABA, suggesting they encode negative regulators of the ABA response. The ABA

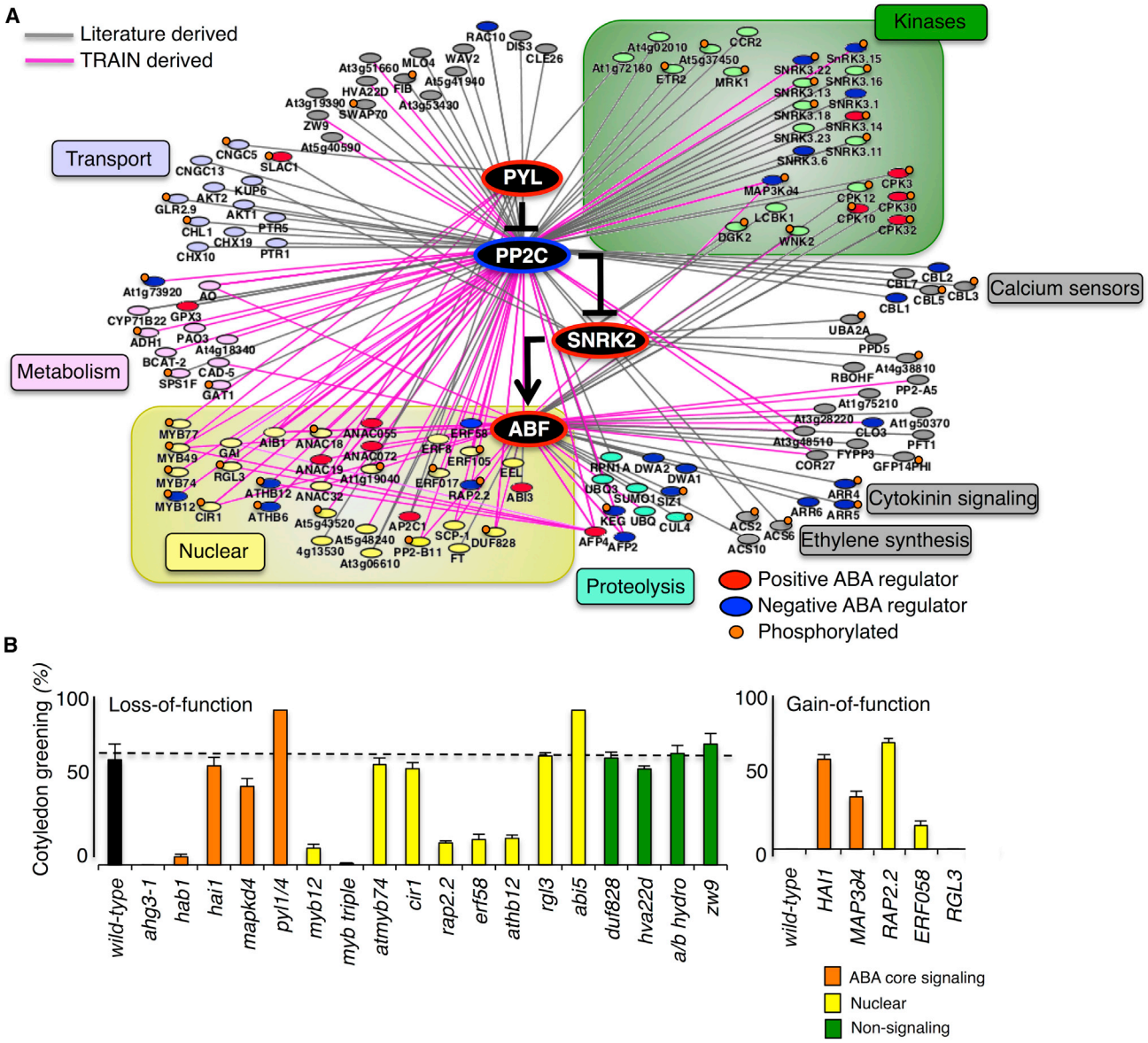

Figure 3. Core ABA Signaling Network

(A) A network of core ABA signaling pathway associations based on the TRAIN and literature-curated interactions. A list of the genes, their partners, and their annotations can be found in Table S1. Gray edges represent previously published core ABA signaling interactions. Pink edges represent interactions found in this study. The ABA core signaling pathway is represented by larger black nodes and arrows. The list of phosphorylated proteins (orange balls) can be found in Table S1. The designation of positive and negative regulators in based on genetic analysis performed in this study or the literature.

(B) Loss- and gain-of-function mutant analysis of select core component partners. Lines were tested on 0.7 μM ABA for hypersensitivity to ABA and 2.0 μM ABA for insensitivity. Three to six independent experiments were performed on each line using 50–100 seeds, and similar results were obtained. The loss-of-function ABA-hypersensitive mutant *ahg3-1* and ABA-insensitive *abi5-1* were used for comparison. For gain-of-function analysis, a strong DEX-inducible line overexpressing *HAI1* was used. Data are represented as mean ± SD.

hypersensitivity of *athb12* is consistent with other studies (Valdés et al., 2012). In addition, the *myb12* triple mutant containing another *myb12* allele in combination with loss-of-function mutations in its closest homologs (*myb12 myb11 myb111*) resulted in an ABA-hypersensitive phenotype (Figure 3B). MYB12 has been implicated as a positive transcriptional regulator of flavonol synthesis (Stracke et al., 2010). This additional ABA-related phenotype suggests this TF impinges on both pigment and hormone signaling. Finally, we assayed the effects of *ERF058*, *RAP2.2*, and MAP3Kδ4 on ABA sensitivity by constructing transgenic lines that conditionally misexpressed these genes. We found that dexamethasone (DEX)-inducible gain-of-function lines for all three transgenics were less sensitive to ABA in the presence of DEX (Figure 3B). These results suggest these genes were both necessary and sufficient negative regulators of ABA responsiveness.

In summary, over 50 interactions to core components have been added from the TRAIN to approximately 60 PPIs curated from the literature. Interestingly, 20 of these interactions included a member in one of six TF families (*MYB*, *HB*, *DELLA*, *ANAC*, *ERF*, *bHLH*). By contrast, only the B3 domain TF ABI3 has been reported to interact with an ABA core component outside of the ABFs (Nakamura et al., 2001). Thus, the conditions used in this study appeared to enrich for TF-based interactions that are missed by other high- and low-throughput interaction studies. Finally, no loss- or gain-of-function lines tested in this study uncovered a positive regulator of ABA response. Previous studies indicate that many genes that interact with core signaling components encode negative regulators of the ABA response (Figure 3A; Table S1). TRAIN-related signaling components, for which an ABA-related phenotype could be identified, appear to add to this list of negative regulators.

An SNRK3 Network That Impinges on ABA Responsiveness

One of our goals in developing a mesoscale ABA signaling network was to generate an experimentally tractable system in order to identify signaling modules. To test this hypothesis, we decided to focus on a subnetwork centered around two kinases, SNRK3.15 and SNRK3.22, that formed two large and overlapping hubs (Figure 4A). The SNRK3 family is of particular interest because members of this group in *Arabidopsis* are implicated in a myriad of plant metabolic and stress responses (Batistič et al., 2012; Coello et al., 2011). Moreover, a number of related SNRK3 proteins interact with known core PP2Cs, ABI1, and ABI2, suggesting that these kinases crosstalk to the core ABA signaling pathway (Batistič et al., 2012; Ohta et al., 2003). Finally, higher resolution interaction mapping (Supplemental Experimental Procedures) revealed that SNRK3 interactions were significantly enriched for TFs compared to other types of partners (Fisher's exact test, $p < 2.8 \times 10^{-6}$) (Figure 4A). Moreover, many of the TF partners of SNRK3 interacted with each other, often resulting in three or four node interaction motifs that are indicative of signaling modules (Zhang et al., 2005).

We used bimolecular fluorescence complementation (BiFC) assays in *Nicotiana benthamiana* to validate a large number of SNRK3 interactions in planta (Walter et al., 2004). Based on 22 Y2H results that included both presence and absence of SNRK3-dependent interactions, 17 (77%) were recapitulated in planta (Figures 4B and S3A–S3D). Green and blue lines indicate Y2H interactions that were recapitulated and not recapitulated by BiFC analysis, respectively. We then decided to study a number of SNRK3-TF interactions in more detail by monitoring protein modification using 2D gel shift assays in yeast. We found that the TFs ATHB6, MYB49, RGL3, ERF058, RAP2.2, and ANAC018 showed shifts in charge and size consistent with protein phosphorylation when coexpressed with a SNRK3 in yeast, as indicated by green lines (Figures 4C and S4A). Blue lines denote the absence of a shift. Finally, both SNRK3s phosphorylated RAP2.2, ATHB6, and ANAC18 in vitro, suggesting that these TFs are direct downstream targets of SNRK3s (Figures 4D and S4B). In summary, the level of reproducibility between the yeast- and plant-based assays indicated that many SNRK3-dependent interactions are of high quality. More importantly, interactions gleaned from the TRAIN could be used as a guide in biochemically based experiments to identify direct targets of SNRK3.15 and/or SNRK3.22.

Our analysis of the SNRK3.15/SNRK3.22 subnetwork suggested these kinases form a signaling module that may have roles in the plant's overall ABA response. A key tenet of a signaling module specifies that perturbing modular components often result in similar phenotypes (Hartwell et al., 1999). SNRK3.22 is a key regulator of a plasma membrane H^+-adenosine triphosphatase (ATPase) function, but there is little suggestion of a role for this kinase in ABA-mediated transcription (Fuglsang et al., 2007). Functional analysis of SNRK3.15 suggests this gene is a negative regulator of ABA response, but paradoxically loss of SNRK3.15 decreases expression of common ABA response genes in the presence of ABA (Qin et al., 2008). The TRAIN suggested these kinases should function in related processes that should connect to ABA-based transcription. To explore this possibility, we first analyzed both loss- and gain-of function alleles of these genes with respect to ABA sensitivity. We found that loss-of-function alleles in both kinases had increased sensitivity to ABA versus wild-type (Figure 4E). Consistent with this, DEX-inducible gain-of-function lines for both of the SNRK3s were less sensitive to ABA in the presence of DEX (Figure 4E). Therefore, *SNRK3.15* and *SNRK3.22* were both necessary and sufficient negative regulators of ABA responsiveness. Next, to clarify the role of SNRK3.15 in ABA-mediated transcription, we activated *SNRK3.15* in our DEX-inducible SNRK3.15 seedlings by DEX addition and monitored genome-wide transcription after ABA treatment (Figure S5). After filtering the data for consistency of expression, approximately 200 genes showed a 2-fold change in expression upon ABA addition in the absence of SNRK3.15 activation (Table S2). Of these, 141 genes were misexpressed in the *snrk2* triple mutant; thus, 70% of the ABA-responsive genes in our data set are influenced by core ABA signaling (Fujita et al., 2009). Upon activation of SNRK3.15, transcription of many of these ABA-responsive genes was attenuated (Figure 4F). This result is consistent with our functional analysis and suggests the SNRK3.15/SNRK2.22 hub plays a role in dampening transcription dependent on core ABA signaling.

Integrative Mapping of the TRAIN by Coexpression Analysis Identifies Putative Abiotic Modules

Whole-genome expression analysis has been used extensively to dissect the role of ABA in the overall response of plants to various stresses such as drought, salt, and temperature (Kilian et al., 2007; Cramer et al., 2011; Zeller et al., 2009). However, animal studies have demonstrated that the performance of transcriptome data as a diagnostic tool of particular processes is greatly improved when expression data are mapped onto protein interaction maps (Taylor et al., 2009; Chuang et al., 2007). This is particularly true when data integration focuses on proteins with many interacting partners ("hubs") as hubs are critical to network conductivity (Fraser, 2005; Han et al., 2004). We therefore decided to combine transcriptome data garnered from a variety of abiotic stresses with the TRAIN to see whether dynamic patterns of network wiring emerge in response to particular stresses.

Rather than simply overlaying the magnitude of expression of TRAIN genes during a specific time or stress condition onto

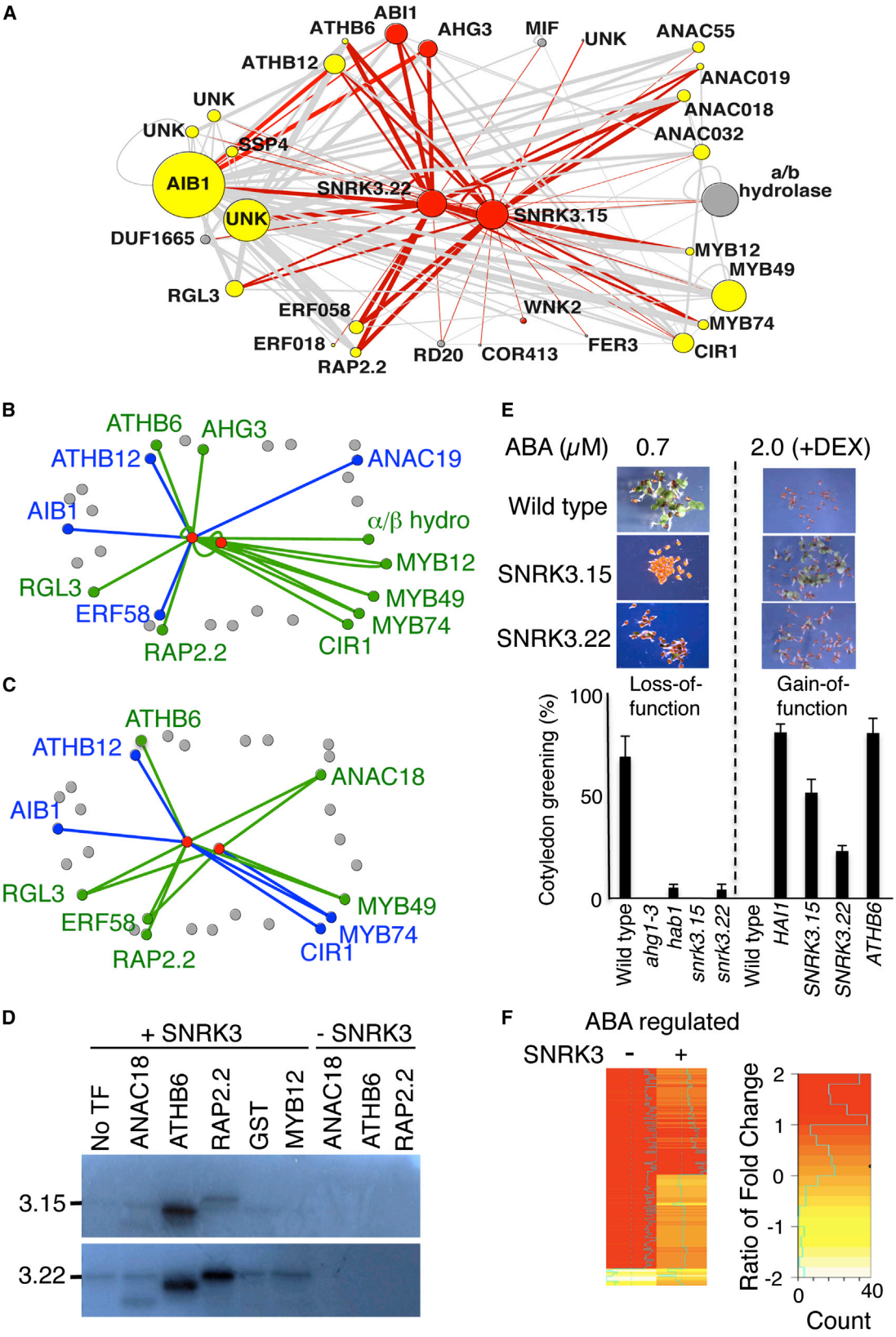

(legend on next page)

TRAIN nodes, we calculated a Pearson correlation coefficient (PCC) of coexpression for each pair of interacting proteins within the TRAIN, across multiple time points for both shoots and roots upon individual stresses. A PCC value above 0.75 reflected high coexpression between the partners, whereas values below −0.75 meant the gene pair is anticorrelated in expression. For example, coexpression analysis based on osmotic stress expression data from combined root and shoot tissues over 12 time points from AtGenExpress generated average PCC values between PYL4 and its PP2C partners of −0.9766 (HAB1), −0.849 (ABI1), −0.8833 (HAI1), and −0.8378 (AHG3) (Kilian et al., 2007). These highly negative correlations are consistent with the diametrically opposed expression of these genes in the presence of ABA.

To evaluate TRAIN coexpression analysis versus standard representations of gene expression globally, we first generated heatmap representations of TRAIN gene expression over the same various abiotic stresses and times (Figure 5A). Osmotic, salt, and cold stress all showed related patterns of gene expression, with osmotic and salt stresses being the most similar. However, although osmotic and salt stresses have similar heatmap expression patterns, their TRAIN coexpression maps showed clear differences (Figure 5B). The HAI1 hub, for example, was highly correlated with the expression of many of its partners in both osmotic and salt stress data sets. But the hub protein MAP3kδ4 only correlated well with its partners under osmotic stress, whereas AIB1 highly correlated with its partners in salt stress (Figure 5B). Neither *MAP3Kδ* nor *AIB1* have been extensively studied, but these results suggest these genes may be associated with these particular stresses.

To explore this possibility in detail, we examined the AIB1 subnetwork. The AIB1 hub represents 55 partners, many of which show highly correlated expression with AIB1 under salt stress conditions (Figure 6A; Table S1). Many of the AIB1 partners that show salt-dependent coexpression are annotated as having roles within the nucleus. After limiting partner interactions to TFs, an AIB1-centered complex comprised of ATHB12 and a collection of ANAC and MYB TFs emerged (Figure 6A). By comparison, similar coexpression analysis based on osmotic expression data did not predict these AIB1 complexes (Figure 6A). By contrast, coexpression analysis identified an osmotic-related complex consisting of ABI5, AFP2, and ATHB12, which were not supported under salt stress conditions (Figure 6A). This analysis suggested different nuclear complexes may coalesce in response to different abiotic stresses and that AIB1 might be a key component of a transient nuclear complex that functions in salt homeostasis. Unfortunately, loss-of-function mutations in the *AIB1* gene are not publically available to test its function. Thus, we constructed DEX-inducible gain-of-function *AIB1* lines and tested them for osmotic- and salt-related phenotypes. The presence of DEX did not influence the growth response of *AIB1* transgenic seedlings to increasing osmotic stress (Figure 6B). By contrast, DEX induction of *AIB1* in transgenic plants did confer an increased sensitivity to salt that was not observed in the absence of DEX, which suggested *AIB1* has a negative role in salt homeostasis (Figure 6B). These results suggest that changes in modularity as monitored by changes in coexpression of protein partners may improve the predictive value of interactomes for designing function experiments.

DISCUSSION

We have developed a systems-based strategy to define a signaling landscape for the plant hormone ABA. Our approach was centered on the premise that proteins contributing to the ABA signaling network will often be coexpressed and should interact at some point to transduce signaling information. Unlike many ABA-based transcriptome studies, we limited our conditions to low levels of ABA and a short duration of exposure to ABA in order to enrich for primary transcriptional events. This resulted in only a few hundred genes whose expression appeared to be regulated mostly by core ABA signaling. This relatively small number of genes allowed meticulous experimental, statistical, and annotation analysis of our protein interaction space to give a high-quality ABA-regulated network of over 500 interactions. Our approach confirmed many core ABA signaling interactions and linked core components to over 50 additional protein partners, many of which represent various transcriptional factor families. The mesoscale nature of the TRAIN also allowed systematic functional analysis of specific signaling modules. And finally, mapping coexpression correlation onto the TRAIN allowed prediction of genes and signaling modules that may play important roles in specific ABA-related abiotic stresses.

Although the TRAIN is an attempt to define a comprehensive ABA signaling network, there are several constraints to our

Figure 4. The SNRK3 Network

(A) The SNRK3.15-SNRK3.22 interaction network. Red connecting lines represent direct SNRK3.15 and SNRK3.22 partners, and gray lines are other protein interactions. Line thickness indicates the edge-weighted confidence based on statistical analysis. Node size is proportional to the total number of interactions in the TRAIN data set.

(B) Summary of BiFC analysis of SNRK3.15 and SNRK3.22 interactions in planta. Green lines are Y2H interactions recapitulated by BiFC; blue lines are Y2H interactions that were not recapitulated by BiFC analysis. See also Figures S3A–S3D.

(C) Summary of 2D gel analysis of TF mobility shifts in the presence of either SNRK3 in yeast. Green lines are SNRK3-dependent shifts, whereas blue lines denote the absence of a shift. See also Figure S4A.

(D) In vitro phosphorylation by SNRK3s of a select number of TF targets. The band observed in the no TF lane is consistent with SNRK3 autophosphorylation. See also Figure S4B.

(E) Loss- and gain-of-function analyses of SNRK3.15 and SNRK3.22 lines. Conditions were similar to those presented in Figure 3B. Quantification of germination and cotyledon expansion of loss- and gain-of-function lines germinated on ABA are shown in the graph. Data are represented as mean ± SD.

(F) Transcriptome analysis of a DEX-inducible SNRK3.15 line in the presence of ABA. Left lane: genes are filtered for those that showed at least a 2-fold increase (red) or decrease (yellow) in the absence of DEX. See also Figure S5 and Table S2. Right lane: expression of the 2-fold gene set in the presence of SNRK3.15 activation. If the expression of an ABA-induced gene is dampened, it becomes more yellow, whereas decreased expression of a repressed gene results in increased red color. Dotted gray line represents 0-fold baseline, whereas the solid line represents the fold change for each gene.

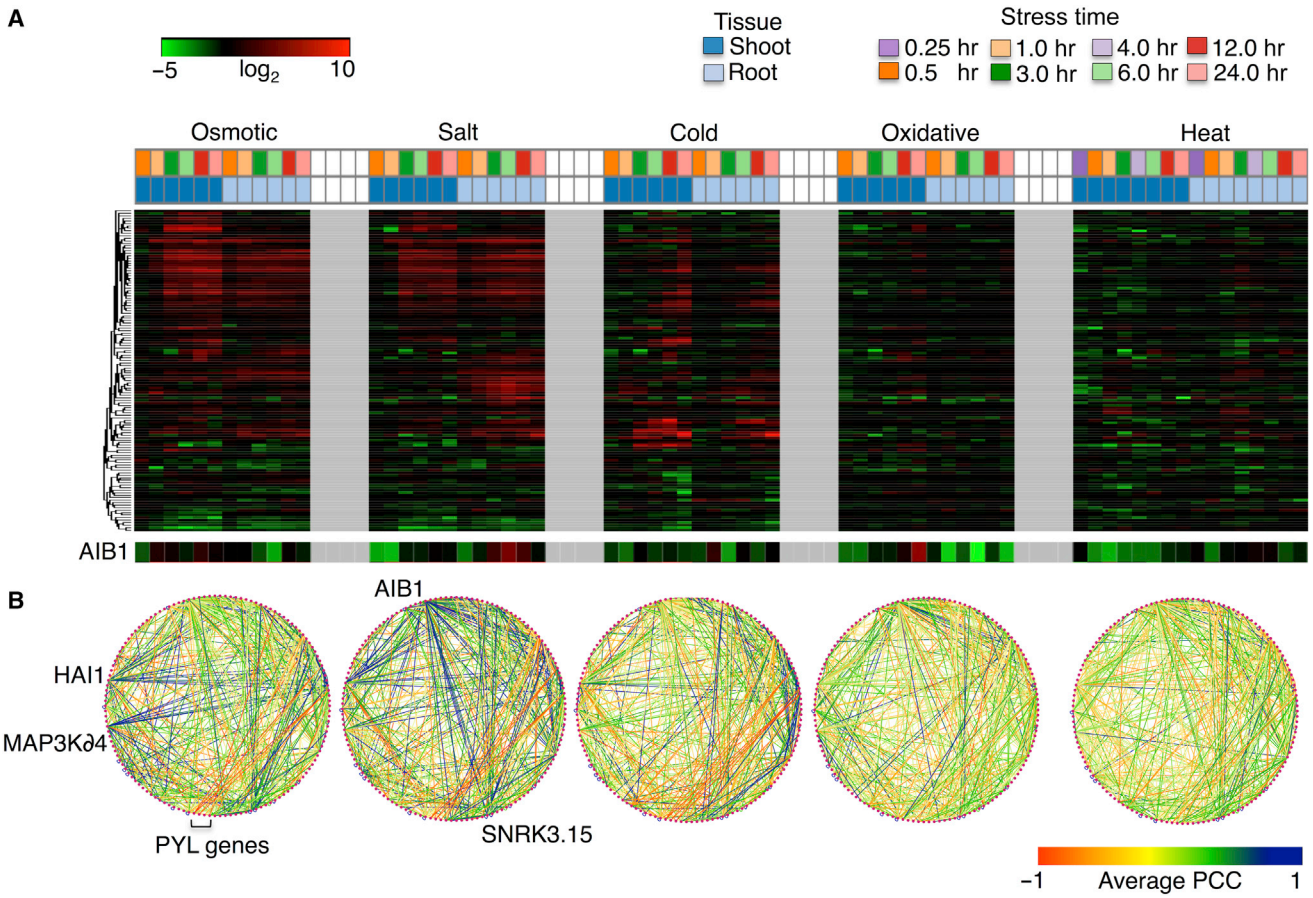

Figure 5. Dynamic Modularity of the TRAIN in Response to Different Abiotic Stresses

(A) Heatmap representation of TRAIN gene expression in the shoot and root under different times of abiotic stress. The lower panel is a magnification of AIB1 expression.

(B) Network graph of the TRAIN with interactions shown as edges that are colored according to the PCC of coexpression of partner proteins. Edge color indicates level of correlation between partner proteins, with bluer edges indicating more correlated coexpression and redder edges indicating more anticorrelation.

approach. First, it is expected that ABA does not transcriptionally regulate many important genes that contribute to its signaling network. For example, the core SNRK2s involved in ABA signaling are not regulated by ABA addition (Fujita et al., 2011). With this in mind, we merged the TRAIN with literature-curated protein interactions (Arabidopsis Interactome Mapping Consortium, 2011; Lalonde et al., 2010; Popescu et al., 2009). This eTRAIN doubled the number of interactions and contained proteins that belong to over 30 GO-annotated functions. Interestingly, although literature curation doubled the size of the interactome, one gene, encoding a LEA protein (At1g65690), actually accounted for over 200 of these additional interactions. Removal of these LEA interactions meant that only 384 interactions out of the 30,000 confirmed PPIs reported for *Arabidopsis* were added to the TRAIN. Moreover, there was little interaction space overlap between the TRAIN and those published for high-throughput studies. These differences may reflect the experimental limitations that are inherent to high-throughput systems, and analysis of high-throughput plant interactomes suggests these approaches have likely captured only 10% of the possible interactions (Chen et al., 2010; Arabidopsis Interactome Mapping Consortium, 2011). By contrast, the medium size of the TRAIN space allows for multiple testing of interactions with different vectors and reporter output systems, which has been shown to be an essential benchmark for quality control in Y2H systems (Chen et al., 2010). The finding that 70% of our Y2H interactions could be recapitulated in planta further supports the experimental and statistical approaches used here to build our interaction network. Whatever the case, the focused approach of this study on a particular process such as hormone signaling is essential in filling out the larger scale interaction maps built by high-throughput methods.

A second limitation of our approach was the use of a specific duration and amount of ABA added, thus limiting our transcriptome analysis to only one stage of development. A recent comprehensive comparison of ABA-regulated transcriptome experiments found few genes in common among 14 data sets (Wang et al., 2011). Although this most likely reflects the differences in ABA concentrations, tissues, and developmental stages used in these experiments, it also demonstrates the flexibility of ABA-related transcriptional response during the life cycle of a higher plant. Thus, a comprehensive ABA network

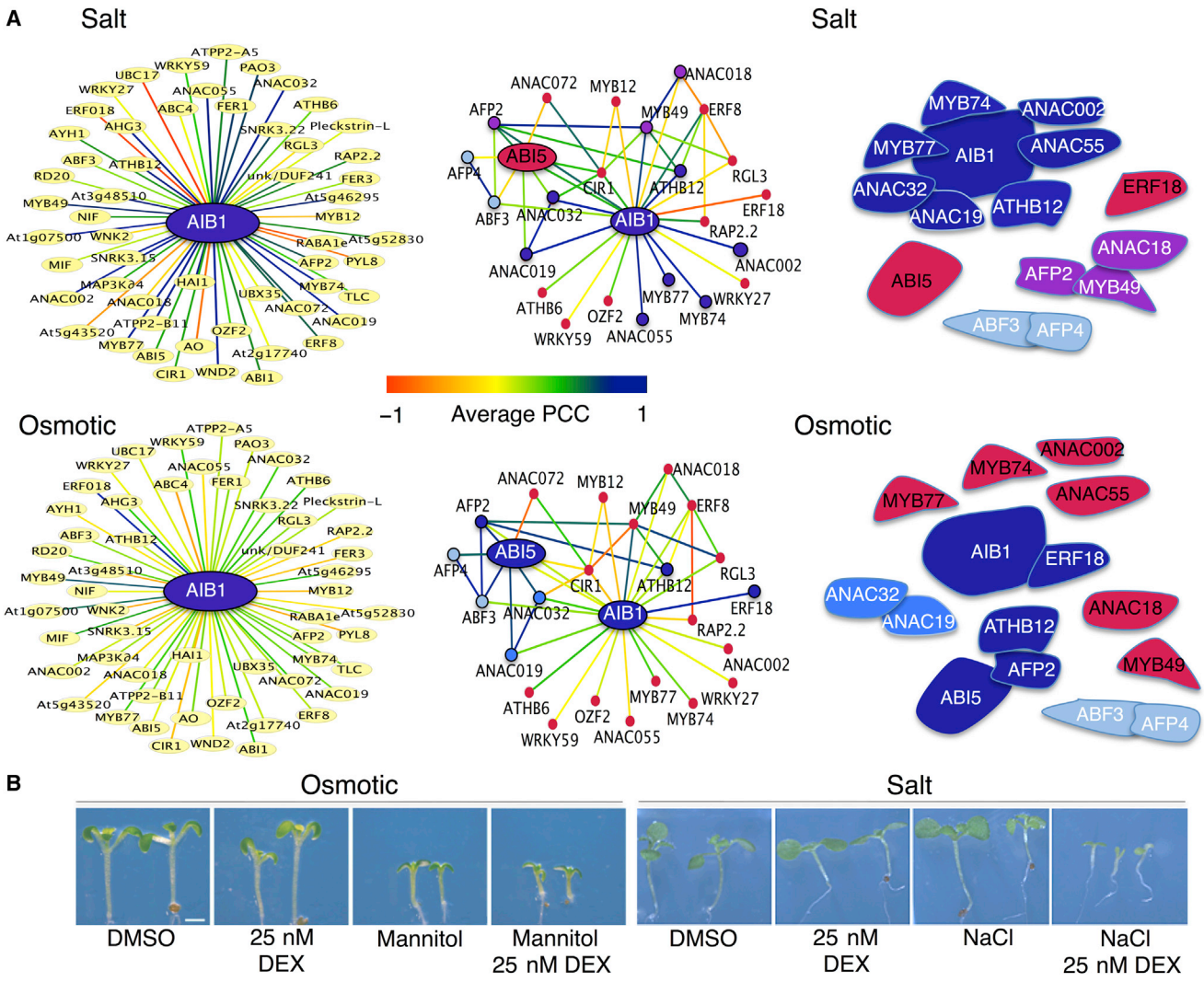

Figure 6. The AIB1 Salt and Osmotic Subnetworks

(A) Left: coexpression analysis of AIB1 partners under salt or osmotic stress. Middle: model of the AIB1 interaction network derived from TF partners. Edge color indicates level of correlation between partner proteins, with bluer edges indicating more correlated coexpression and redder edges indicating more anti-correlation. Right: model of nuclear AIB1 complexes based on coexpression of partners.

(B) Effects of mannitol (1%–5%) and NaCl (25–300 mM) on DEX-inducible *AIB1* transgenic seedlings. Representative pictures are of seedlings grown in the absence (DMSO) or presence of mannitol (5%) or salt (50 mM NaCl) for 7 days. Scale bar, 1.0 mm.

will likely require a number of spatially and temporally based "TRAIN-like" interactomes. The TRAIN could also be reduced to the resolution of a single cell, based on the integration of cell-type specific interaction and expression data. This microscopic level of analysis was not possible prior to the TRAIN and will likely lead to valuable insight into the mechanisms of how different cell types respond to ABA.

It is notable that functional analysis of the TRAIN uncovered only negative regulators of ABA-mediated signaling. This could mean the transcriptome assay conditions used to identify TRAIN genes enriched for negative regulators. However, we think this is unlikely because two-thirds of the genes curated from the literature that link to the core ABA signaling pathway and show ABA-related phenotypes also appear to attenuate the ABA response. This attenuation of the core ABA signaling pathway could reflect a negative feedback response to the initial activation of the core pathway by ABA.

With respect to the ABA signaling network, a large number of kinases annotated as being involved in calcium-mediated signaling appeared to interact with core ABA signaling components and PP2Cs in particular. Within the TRAIN, there were three major kinase hubs: a MAP3Kδ4 and two SNRK3s. Regarding SNRK3.15 and SNRK3.22, our analysis indicated these kinases act as negative regulators of the ABA response, which is opposite to the SNRK2 kinases involved in core ABA signaling (Fujita et al., 2009; Fujii and Zhu, 2009). Interestingly, it appears that a number of TFs interacting with SNRK3(s), including TFs shown to be phosphorylated by either SNRK3.15 or SNRK3.22, were also negative regulators of the ABA response. This could mean these kinases and a number of their

TF targets may form a signaling module. At this time, it is not clear how these SNRK3s coordinate with core SNRK2s to modulate the overall ABA response. SNRK3 transcription is dependent on SNRK2 activation; thus, each kinase group is temporally separated. Furthermore, the absence of SNRK3 interactions with either ABI5 or ABF3 suggests a separation between the TFs regulated by SNRK2s in the core pathway and TFs targeted by SNRK3s. Interestingly, a number of TF partners of SNRK3 interacted with the central ABA signaling transcriptional regulator ABI5 (Lopez-Molina et al., 2001, 2002). Possibly, ABI5 may act as a common point of crosstalk between SNRK2 and SNRK3 signaling.

Although little is known about the targets of SNRK3.15 signaling, SNRK3.22 does negatively regulate the activity of the AHA2 plasma membrane H^+-ATPase through phosphorylation (Fuglsang et al., 2007). The control of plasma membrane H^+-ATPase by SNRK3.22 regulates intracellular pH homeostasis in response to alkaline pH, which in turn modulates the plant's overall response to salt stress under alkaline conditions. Apart from its role in membrane-based salt homeostasis, we found that one target of SNRK3.22, the bHLH TF AIB1, is also connected to a salt stress response. Notably, many SNRK3.15 (24/26) and SNRK3.22 (22/23) interactors also partner with AIB1 (Figure S6). Thus, SNRK3.22 and perhaps SNRK3.15 may act as central coordinators in response to salt stress at both the plasma membrane and the nucleus.

In conclusion, it is believed that most signaling modules are mesoscale, encompassing 25–100 proteins (Spirin and Mirny, 2003). The experimental conditions used in this study, which result in an interaction space around approximately 100 proteins, were ideal in capturing a network of this scale. Our network was simple enough to identify modules that could be probed functionally. More importantly, unlike other plant studies that identify subnetworks through functional analysis or gene expression signatures alone, the overlaying of coexpression onto the TRAIN led to the identification of dynamic subnetworks based on changes in network wiring. These changes in subnetworks can be used to determine functional roles for hubs and specific signaling modules. We believe this approach of merging coexpression onto protein interaction networks will have important predictive value in assigning gene function. On this note, the approaches used here should be readily applicable to other mesoscale signaling processes such as pathogen infection or growth on different nutrient conditions. These approaches would also be advantageous in dissecting nonmodel plant and animal processes where genetic tools are not readily available.

EXPERIMENTAL PROCEDURES

Plant Material and Growth Conditions

All *Arabidopsis* strains used in this study were of the ecotype Columbia (Col-0). See Supplemental Experimental Procedures for details.

Construction of the Transcriptionally Regulated ABA Interactome Network

Sterile seeds were placed on 1/2× Murashige-Skoog (MS) plates and imbibed for 4 days at 4°C. Plates were transferred to room temperature under continuous white light for 11 days. Eleven-day-old seedlings were moved to 1/2× MS plates (10 μM cycloheximide ± 1 μM ABA) for 6 hr. Total RNA was processed and hybridized on a GeneChip *Arabidopsis* ATH1 genome array. Duplicate samples were analyzed for each condition. See Supplemental Experimental Procedures for construction of the TRAIN.

Protein Purification and Kinase Assays

Kinase reactions were conducted in 20 μl of kinase buffer with 1 μCi of γ-[^{32}P] ATP for 15 min at room temperature and terminated by adding Laemmli buffer. Reactions were loaded onto 12% SDS-PAGE gels, and incorporated radiolabel was visualized by autoradiography. Kinase assays were run on SDS-PAGE gels and visualized by Coomassie blue staining. See Supplemental Experimental Procedures for details.

Yeast Expression and 2D Gel Analysis

Streaked haploid EGY48 yeast expressing the various TFs in the pJG4-5 vector, or diploid yeast (EGY48/RFY206) coexpressing individual TFs and kinases in the pJG4-5 and pEG202 vectors, respectively, were resuspended from yeast nitrogen base (YNB) plates to 0.1 optical density 600 (OD_{600}) in 3 ml of appropriate YNB galactose drop-out media to induce protein expression. Cultures were grown overnight at 30°C. Pellets were solubilized with glass beads in 200 μl of the rehydration buffer (Bio-Rad), and 75 μg of each protein sample was absorbed into 7 cm Immobilized pH gradient (IPG) (pH 3–10) strips and separated in the first dimension by the Protean IEF Cell per the manufacturer's instructions (Bio-Rad). The IPG strips were processed, and the proteins were separated in the second dimension by 12% SDS-PAGE. Following electrophoresis, the TFs were detected by immunoblot analysis using hemagglutinin antibodies (Roche; 1/15,000).

Bimolecular Fluorescence Complementation Analysis

BiFC and split yellow fluorescent protein (YFP) fusions were transiently expressed using *Agrobacterium tumefaciens* in *N. benthamiana* as described previously (Walter et al., 2004). The *A. tumefaciens* strain GV2260 (final density of 0.2 OD_{600}) was used to syringe-infiltrate *N. benthamiana* leaves. YFP was visualized using standard techniques on a Leica TCS SP5 confocal microscope.

Microarray Analysis of DEX-Inducible *SNRK3.15* Lines

Stratified seeds were transferred to room temperature under continuous white light for 4 days and then transferred to either a 0.1% DMSO or a 30 μM DEX plate (24 hr). After this incubation, seeds were transferred to 0.1% DMSO or 2 μM ABA ± 30 μM DEX for 24 hr. RNA was analyzed by hybridization on a GeneChip *Arabidopsis* ATH1 genome array. See Supplemental Experimental Procedures.

Gene Expression Analysis

Gene expression data were generated from the AtGenExpress global stress expression data set downloaded from the Bio-Analytic Resource (http://dx.doi.org/10.1111/j.1365-313X.2005.02437.x) or from Gene Expression Omnibus (Toufighi et al., 2005). The expression platform used in all cases was the ATH1 GeneChip from Affymetrix. The data sets and comparisons were as follows: *aba2-2* seedlings one comparison: 6 hr with 1 μM ABA versus mock-treated plant (http://bar.utoronto.ca/affydb/cgi-bin/affy_db_proj_viewer.cgi?proj=26&view=general). Heatmaps of abiotic stress transcription were generated using GENE-E (http://www.broadinstitute.org/cancer/software/GENE-E/index.html). PCCs between each protein pair within the TRAIN were generated over each abiotic stress using AtGenExpress global stress expression data set expression data from both roots and shoots over six time periods.

SUPPLEMENTAL INFORMATION

Supplemental Information includes Supplemental Experimental Procedures, six figures, and two tables and can be found with this article online at http://dx.doi.org/10.1016/j.devcel.2014.04.004.

ACKNOWLEDGMENTS

We thank Dr. E. Nambara for helpful discussion. We also thank the Ohio State Stock Center and Salk Institute Genomic Analysis Laboratory (SIGnAL) for

providing materials, and Dr. N. Nishimura for *ahg3-1* seed and Dr. Bernd Weisshaar for *myb12* and *myb12 myb11 myb111* triple mutant seed.

Received: October 18, 2013
Revised: February 21, 2014
Accepted: April 1, 2014
Published: May 12, 2014

REFERENCES

Arabidopsis Interactome Mapping Consortium (2011). Evidence for network evolution in an Arabidopsis interactome map. Science *333*, 601–607.

Batistič, O., Rehers, M., Akerman, A., Schlücking, K., Steinhorst, L., Yalovsky, S., and Kudla, J. (2012). S-acylation-dependent association of the calcium sensor CBL2 with the vacuolar membrane is essential for proper abscisic acid responses. Cell Res. *22*, 1155–1168.

Ben-Ari, G. (2012). The ABA signal transduction mechanism in commercial crops: learning from Arabidopsis. Plant Cell Rep. *31*, 1357–1369.

Brandt, B., Brodsky, D.E., Xue, S., Negi, J., Iba, K., Kangasjärvi, J., Ghassemian, M., Stephan, A.B., Hu, H., and Schroeder, J.I. (2012). Reconstitution of abscisic acid activation of SLAC1 anion channel by CPK6 and OST1 kinases and branched ABI1 PP2C phosphatase action. Proc. Natl. Acad. Sci. USA *109*, 10593–10598.

Chen, Y.C., Rajagopala, S.V., Stellberger, T., and Uetz, P. (2010). Exhaustive benchmarking of the yeast two-hybrid system. Nat. Methods *7*, 667–668, author reply 668.

Chuang, H.Y., Lee, E., Liu, Y.T., Lee, D., and Ideker, T. (2007). Network-based classification of breast cancer metastasis. Mol. Syst. Biol. *3*, 140.

Coello, P., Hey, S.J., and Halford, N.G. (2011). The sucrose non-fermenting-1-related (SnRK) family of protein kinases: potential for manipulation to improve stress tolerance and increase yield. J. Exp. Bot. *62*, 883–893.

Cramer, G.R., Urano, K., Delrot, S., Pezzotti, M., and Shinozaki, K. (2011). Effects of abiotic stress on plants: a systems biology perspective. BMC Plant Biol. *11*, 163.

Cutler, S.R., Rodriguez, P.L., Finkelstein, R.R., and Abrams, S.R. (2010). Abscisic acid: emergence of a core signaling network. Annu. Rev. Plant Biol. *61*, 651–679.

Fraser, H.B. (2005). Modularity and evolutionary constraint on proteins. Nat. Genet. *37*, 351–352.

Fuglsang, A.T., Guo, Y., Cuin, T.A., Qiu, Q., Song, C., Kristiansen, K.A., Bych, K., Schulz, A., Shabala, S., Schumaker, K.S., et al. (2007). Arabidopsis protein kinase PKS5 inhibits the plasma membrane H+-ATPase by preventing interaction with 14-3-3 protein. Plant Cell *19*, 1617–1634.

Fujii, H., and Zhu, J.-K. (2009). Arabidopsis mutant deficient in 3 abscisic acid-activated protein kinases reveals critical roles in growth, reproduction, and stress. Proc. Natl. Acad. Sci. USA *106*, 8380–8385.

Fujita, Y., Nakashima, K., Yoshida, T., Katagiri, T., Kidokoro, S., Kanamori, N., Umezawa, T., Fujita, M., Maruyama, K., Ishiyama, K., et al. (2009). Three SnRK2 protein kinases are the main positive regulators of abscisic acid signaling in response to water stress in Arabidopsis. Plant Cell Physiol. *50*, 2123–2132.

Fujita, Y., Fujita, M., Shinozaki, K., and Yamaguchi-Shinozaki, K. (2011). ABA-mediated transcriptional regulation in response to osmotic stress in plants. J. Plant Res. *124*, 509–525.

Garcia, M.E., Lynch, T., Peeters, J., Snowden, C., and Finkelstein, R. (2008). A small plant-specific protein family of ABI five binding proteins (AFPs) regulates stress response in germinating Arabidopsis seeds and seedlings. Plant Mol. Biol. *67*, 643–658.

Ge, H., Liu, Z., Church, G.M., and Vidal, M. (2001). Correlation between transcriptome and interactome mapping data from *Saccharomyces cerevisiae*. Nat. Genet. *29*, 482–486.

Geiger, D., Maierhofer, T., Al-Rasheid, K.A., Scherzer, S., Mumm, P., Liese, A., Ache, P., Wellmann, C., Marten, I., Grill, E., et al. (2011). Stomatal closure by fast abscisic acid signaling is mediated by the guard cell anion channel SLAH3 and the receptor RCAR1. Sci. Signal. *4*, ra32.

Han, J.D., Bertin, N., Hao, T., Goldberg, D.S., Berriz, G.F., Zhang, L.V., Dupuy, D., Walhout, A.J., Cusick, M.E., Roth, F.P., and Vidal, M. (2004). Evidence for dynamically organized modularity in the yeast protein-protein interaction network. Nature *430*, 88–93.

Hartwell, L.H., Hopfield, J.J., Leibler, S., and Murray, A.W. (1999). From molecular to modular cell biology. Nature *402* (6761, Suppl), C47–C52.

Hey, S.J., Byrne, E., and Halford, N.G. (2010). The interface between metabolic and stress signalling. Ann. Bot. (Lond.) *105*, 197–203.

Huang, G.T., Ma, S.L., Bai, L.P., Zhang, L., Ma, H., Jia, P., Liu, J., Zhong, M., and Guo, Z.F. (2012). Signal transduction during cold, salt, and drought stresses in plants. Mol. Biol. Rep. *39*, 969–987.

Hubbard, K.E., Nishimura, N., Hitomi, K., Getzoff, E.D., and Schroeder, J.I. (2010). Early abscisic acid signal transduction mechanisms: newly discovered components and newly emerging questions. Genes Dev. *24*, 1695–1708.

Kilian, J., Whitehead, D., Horak, J., Wanke, D., Weinl, S., Batistic, O., D'Angelo, C., Bornberg-Bauer, E., Kudla, J., and Harter, K. (2007). The AtGenExpress global stress expression data set: protocols, evaluation and model data analysis of UV-B light, drought and cold stress responses. Plant J. *50*, 347–363.

Lalonde, S., Sero, A., Pratelli, R., Pilot, G., Chen, J., Sardi, M.I., Parsa, S.A., Kim, D.Y., Acharya, B.R., Stein, E.V., et al. (2010). A membrane protein/signaling protein interaction network for Arabidopsis version AMPv2. Front. Physiol. *1*, 24.

Léon-Kloosterziel, K.M., Gil, M.A., Ruijs, G.J., Jacobsen, S.E., Olszewski, N.E., Schwartz, S.H., Zeevaart, J.A., and Koornneef, M. (1996). Isolation and characterization of abscisic acid-deficient Arabidopsis mutants at two new loci. Plant J. *10*, 655–661.

Li, H.H., Hao, R.L., Wu, S.S., Guo, P.C., Chen, C.J., Pan, L.P., and Ni, H. (2011). Occurrence, function and potential medicinal applications of the phytohormone abscisic acid in animals and humans. Biochem. Pharmacol. *82*, 701–712.

Lopez-Molina, L., Mongrand, S., and Chua, N.H. (2001). A postgermination developmental arrest checkpoint is mediated by abscisic acid and requires the ABI5 transcription factor in Arabidopsis. Proc. Natl. Acad. Sci. USA *98*, 4782–4787.

Lopez-Molina, L., Mongrand, S., McLachlin, D.T., Chait, B.T., and Chua, N.H. (2002). ABI5 acts downstream of ABI3 to execute an ABA-dependent growth arrest during germination. Plant J. *32*, 317–328.

Lumba, S., Cutler, S., and McCourt, P. (2010). Plant nuclear hormone receptors: a role for small molecules in protein-protein interactions. Annu. Rev. Cell Dev. Biol. *26*, 445–469.

Lynch, T., Erickson, B.J., and Finkelstein, R.R. (2012). Direct interactions of ABA-insensitive(ABI)-clade protein phosphatase(PP)2Cs with calcium-dependent protein kinases and ABA response element-binding bZIPs may contribute to turning off ABA response. Plant Mol. Biol. *80*, 647–658.

Nakamura, S., Lynch, T.J., and Finkelstein, R.R. (2001). Physical interactions between ABA response loci of Arabidopsis. Plant J. *26*, 627–635.

Nakashima, K., and Yamaguchi-Shinozaki, K. (2013). ABA signaling in stress-response and seed development. Plant Cell Rep. *32*, 959–970.

Ohta, M., Guo, Y., Halfter, U., and Zhu, J.-K. (2003). A novel domain in the protein kinase SOS2 mediates interaction with the protein phosphatase 2C ABI2. Proc. Natl. Acad. Sci. USA *100*, 11771–11776.

Park, S.Y., Fung, P., Nishimura, N., Jensen, D.R., Fujii, H., Zhao, Y., Lumba, S., Santiago, J., Rodrigues, A., Chow, T.F., et al. (2009). Abscisic acid inhibits type 2C protein phosphatases via the PYR/PYL family of START proteins. Science *324*, 1068–1071.

Popescu, S.C., Popescu, G.V., Bachan, S., Zhang, Z., Gerstein, M., Snyder, M., and Dinesh-Kumar, S.P. (2009). MAPK target networks in *Arabidopsis thaliana* revealed using functional protein microarrays. Genes Dev. *23*, 80–92.

Qin, Y., Li, X., Guo, M., Deng, K., Lin, J., Tang, D., Guo, X., and Liu, X. (2008). Regulation of salt and ABA responses by CIPK14, a calcium sensor interacting protein kinase in Arabidopsis. Sci. China C Life Sci. *51*, 391–401.

Spirin, V., and Mirny, L.A. (2003). Protein complexes and functional modules in molecular networks. Proc. Natl. Acad. Sci. USA *100*, 12123–12128.

Stelzl, U., Worm, U., Lalowski, M., Haenig, C., Brembeck, F.H., Goehler, H., Stroedicke, M., Zenkner, M., Schoenherr, A., Koeppen, S., et al. (2005). A human protein-protein interaction network: a resource for annotating the proteome. Cell *122*, 957–968.

Stracke, R., Jahns, O., Keck, M., Tohge, T., Niehaus, K., Fernie, A.R., and Weisshaar, B. (2010). Analysis of production of flavonol glycosides-dependent flavonol glycoside accumulation in *Arabidopsis thaliana* plants reveals MYB11-, MYB12- and MYB111-independent flavonol glycoside accumulation. New Phytol. *188*, 985–1000.

Taylor, I.W., Linding, R., Warde-Farley, D., Liu, Y., Pesquita, C., Faria, D., Bull, S., Pawson, T., Morris, Q., and Wrana, J.L. (2009). Dynamic modularity in protein interaction networks predicts breast cancer outcome. Nat. Biotechnol. *27*, 199–204.

Toufighi, K., Brady, S.M., Austin, R., Ly, E., and Provart, N.J. (2005). The Botany Array Resource: e-Northerns, Expression Angling, and promoter analyses. Plant J. *43*, 153–163.

Valdés, A.E., Overnäs, E., Johansson, H., Rada-Iglesias, A., and Engström, P. (2012). The homeodomain-leucine zipper (HD-Zip) class I transcription factors ATHB7 and ATHB12 modulate abscisic acid signalling by regulating protein phosphatase 2C and abscisic acid receptor gene activities. Plant Mol. Biol. *80*, 405–418.

Van Leene, J., Boruc, J., De Jaeger, G., Russinova, E., and De Veylder, L. (2011). A kaleidoscopic view of the Arabidopsis core cell cycle interactome. Trends Plant Sci. *16*, 141–150.

Walter, M., Chaban, C., Schütze, K., Batistic, O., Weckermann, K., Näke, C., Blazevic, D., Grefen, C., Schumacher, K., Oecking, C., et al. (2004). Visualization of protein interactions in living plant cells using bimolecular fluorescence complementation. Plant J. *40*, 428–438.

Wang, R.S., Pandey, S., Li, S., Gookin, T.E., Zhao, Z., Albert, R., and Assmann, S.M. (2011). Common and unique elements of the ABA-regulated transcriptome of Arabidopsis guard cells. BMC Genomics *12*, 216.

Wasilewska, A., Vlad, F., Sirichandra, C., Redko, Y., Jammes, F., Valon, C., Frei dit Frey, N., and Leung, J. (2008). An update on abscisic acid signaling in plants and more. Mol. Plant *1*, 198–217.

Wilkinson, S., Kudoyarova, G.R., Veselov, D.S., Arkhipova, T.N., and Davies, W.J. (2012). Plant hormone interactions: innovative targets for crop breeding and management. J. Exp. Bot. *63*, 3499–3509.

Yu, H., Braun, P., Yildirim, M.A., Lemmens, I., Venkatesan, K., Sahalie, J., Hirozane-Kishikawa, T., Gebreab, F., Li, N., Simonis, N., et al. (2008). High-quality binary protein interaction map of the yeast interactome network. Science *322*, 104–110.

Zeller, G., Henz, S.R., Widmer, C.K., Sachsenberg, T., Rätsch, G., Weigel, D., and Laubinger, S. (2009). Stress-induced changes in the Arabidopsis thaliana transcriptome analyzed using whole-genome tiling arrays. Plant J. *58*, 1068–1082.

Zhang, L.V., King, O.D., Wong, S.L., Goldberg, D.S., Tong, A.H., Lesage, G., Andrews, B., Bussey, H., Boone, C., and Roth, F.P. (2005). Motifs, themes and thematic maps of an integrated Saccharomyces cerevisiae interaction network. J. Biol. *4*, 6.